Predicting Vibrational Mean Free Paths and Thermal Conductivity Accumulations for Amorphous Materials

Jason M. Larkin[1] and Alan J. H. McGaughey[1]

[1]*Department of Mechanical Engineering*
Carnegie Mellon University
Pittsburgh, PA 15213

(Dated: June 18, 2013)

Understanding thermal transport in crystalline systems requires detailed knowledge of phonons, which are the quanta of energy associated with atomic vibrations. By definition, phonons are non-localized vibrations that transport energy over distances much larger than the atomic spacing. For disordered materials (e.g., alloys, amorphous phases), with the exception of very long wavelength modes, the vibrational modes are localized and do not propagate like phonons. The Einstein model assumes that the mean free path of these localized vibrations is the average interatomic distance and that their group velocity is equal to the speed of sound. The Cahill-Pohl model assumes that the mean free path of the localized modes is equal to half of their wavelength. While these approach can be used to estimate the thermal conductivity of disordered systems, they only provide a qualitative description of the vibrations that contribute to the lattice thermal conductivity. Using lattice dynamics calculations and molecular dynamics simulations on model amorphous silicon and silica, we predict and characterize the contributions from phonons and localized vibrations to lattice thermal conductivity. The vibrational mean free paths are predicted for these two amorphous materials and the thermal conductivity accumulation function is compared with recent experimental results.

I. INTRODUCTION

Thermal transport, MFPs

Thermal transport at scales comparable to phonon wave- lengths and mean free paths (MFPs) is presently a topic of considerable interest [14].[1–4]

Recently, nanostructured materials such as nanowires, superlattices, and nanocomposites with strongly reduced thermal conductivities due to phonon scattering at interfaces and boundaries have been reported and are being considered for use in thermoelectrics applications.[3–6] Recent empirical and first-principles calculations show that MFPs of phonons relevant to thermal conduc- tivity vary by more than 5 orders of magnitude in crystalline materials.[7] Traditionally, empirical expressions and simple relaxation time models have been the only means to estimate MFPs [11].[8]

The thermal conductivity of amorphous solids display unique temperature dependance compared to ordered solids.[9] Cahill argued that the lattice vibrations in a disordered crystal are essentially the same as those of an amorphous solid.[10]

Non-local

Another type of size effect can occur if there is a temperature gradient over length scales compa- rable to phonon MFPs. In this case, local thermal equilibrium does not exist and the transport is nondiffusive. Transient ballistic transport has been studied using heat-pulse techniques at cryogenic temperatures [8].[?] A non-local theory of heat transport was proposed as a modification of diffusion theory [9].[11] It was also predicted that the heat conduction from a nanoparticle is significantly reduced from the Fourier law prediction.[12]

Experimental

Broadband Techniques

Experimentally, inelastic neutron scattering has been used to measure phonon lifetimes in certain materials, but this technique is more suited for single crystal samples [13].[13] Koh et al. proposed a technique which uses a variation of modulation frequency to measure MFPs, but this technique is limited by the modulation frequency [15].[14] An x-ray diffraction and thermoreflectance technique can measure ballistic transport in some structures [14].[15]

The understanding of the accumulation function for bulk crystalline has made significant advancement experimentally[16] and theoretically.[17] However, understanding of accumulation in amorphous systems is still not well understood.[18–20] recent measurements of the accumulation function by Regner .[21]

Film Thickness Dependance

Measurements of the thermal condutivity of a-SiO_2 thin films show no significant dependance on the film thickness.[22,23] Measurements by all the refs from Galli paper, showing strong dependance on film thickness.[24–30]

a-Si

[24] find 1.8 W/m-K, similar to the SW results presented here. Yang et al find as high as 6 W/m-K.[26] Liu et al. find a film dependanc between 60 and 80 microns.[30] Claim the HWCVD method and hydrogenation creates the most ordered a-Si. zink shows no plateau at low T for a-Si thin film, indicating the scattering of long-wavelength phonon-like modes by the boundaries.[25] Show film thickness dependance up to 10 microns.[28] 4.8

W/m-K.[31]

A. Low-frequency Scalings: w4 vs w2

B. w4

w4: as predicted for phonons scattering off point defects under the Debye approximation.

Initial work by Zeller and Pohl[32] and later by Grabner et al.[33] demonstrated that the low-frequency, long-wavelength vibrations in glasses that dominate at low temperature can be characterized using Rayleigh type scattering, $\Lambda \propto \omega^{-4}$.

Experimental measurements of linewdiths in a-SiO2 seemed to be explained by Rayleigh scattering.[34] However, in a separate experiment on a-SiO2, a cross-over from w2, to w4, and back to w2 was observed.[35] Theory from Schirmacher et al. predicted an w4 scaling below a system dependent onset frequency.[36,37] Another experiment reported Rayleigh-like scattering (and even stronger) while demonstrating that w2-like scaling can be mistaken by considering large intervals of frequency and wavelength.[38]

sound-wave scattering in a-SiO_2 shows Rayleigh type[34] numerical study of disordered lattices with varying coordination show Rayleigh type scattering.[39]

C. w2

w2: as predicted for phonons scattering off other phonon, where the Debye approximation is often used.

Low temperature conductivity and specific heat measurements demonstrate that the propagating modes in a-Si and doped a-Si follow $\Lambda \propto \omega^{-2}$.[25?]

Fabian and Allen predict w2 dependance for model of a-Si.[40]

shows $\tau\ \omega^{-2}$ for a hard-sphere model.[41] shows w2 scaling of the inverse linewdiths from structure factor of model glasses.[42] shows w2 for long, w2.5 for tran for a model of a-SiO2.[43]

review paper on aiSO2: models and experimental data for a-SiO2 shows w2 for short wavelength, high frequency modes and scaling near w2.5 at low frequency.[44]

Using theory based on the random spatial variation of the shear modulus, a transition from w4 to w2 scaling is observed at frequencies much lower than the so-called "Boson peak" frequency.[37]

experiment from Benassi et al. show a k^2 dependance.[45]

Experimentally, for Q larger than 1 nm 1 , all glasses studied so far show $\tau \propto k^x$, with x very close to 2, see Ref. 35 for a review.

a-Si Christie et al. find a best fit of w2.5 for a model of a-Si, although adequate fits to w2 and w4 were shown.[46]

The nature of vibrations in amorphous systems in this frequency region is not yet fully understood. It is known that a force-constant-disordered crystalline lattice gives w4,[47,48] while many positionally disordered materials, including a-Si, give w2, as does a positionally disordered analytical model.[49,50]

It may therefore be positional disorder which is responsible for the reduction in the exponent from 4 to 2, although the mechanism of this reduction remains unclear. Of particular interest is the recent experimental work of Masciovecchio et al.,[35] which suggests that there may be three regimes in vitreous silica, with respectively w2 to w4 and back to w2. If this behavior is generally true, then these regions could occur at different ranges of wavevector for different materials, and this could account for different dependences being observed between different materials; the w4 dependence in lithium diborate,[38] and for the intermediate value of exponent 2.54 found for the transverse polarization by Christie et al.[46] and others.

In conclusion we have shown that in a system without any periodic order such as a monatomic liquid, one observes in- elastic excitations that can be interpreted as the noncrystal- line counterpart of Umklapp peaks.[?]

The goal of this work...

In this work, we consider two "stiff glass" amorphous systems: Structural relxation phenomena do not dominate the dynamics of the.[41]

For modeling the low frequency vibrational modes, two types of scattering mechanisms are considered: (a) phonon-phonon scattering (b) Rayleigh scattering.

The vibrational modes in these systems are characterized in the limit of propagating (phonon) and non-propagating (diffuson) modes by predicting the mode lifetimes and estimating their mean free paths. The spectrum of vibrational MFPs and the accumulated thermal conductivity are predicted for a-SiO2 and a-Si. The dominant heat carriers in a-SiO_2 are shown to be diffusons: non-propagating vibrational modes which carry a significant amount of heat. For a-Si, ...

II. THEORETICAL FORMULATION

A. Vibrational Thermal Conductivity

To calculate the total vibrational thermal conductivity k_{vib} of a disordered system, we predict the contributions from k_{ph} and k_{AF},

$$k_{vib} = k_{ph} + k_{AF}, \tag{1}$$

where k_{ph}[?] is the contribution from phonons or phonon-like modes and k_{AF} is the contribution from the Allen-Feldman theory of diffusons.[18,19] A study of disordered Lennard-Jones argon and Stillinger-Weber silicon lattices demonstrated that k_{AF} is a significant fraction of k_{vib}, even when spatial disorder is not included. For amorphous systems, the spatial disorder creates strong scattering, and k_{vib} tends to be much smaller than the crystalline phase.(cite)

The relative contribution of k_{ph} and k_{AF} to k_{vib} has been estimated to be approximately equal for a model of a-Si at 300 K,[51] while earlier studies find that k_{ph} is less than half.[18,19] Experimental measurements and estimates show that the contribution from k_{ph} is 40%.[30]

The themal conductivity of a-GeTe[52] The thermal conductivity of silicon nanowires[53]

To calculate the total vibrational thermal conductivity k_{vib}, we predict the contributions from k_{ph} and k_{AF}. We use a Debye model for k_{ph}(cite) and the Allen-Feldman theory of diffusons for k_{AF}[18,19] The phonon contribution is

$$k_{ph} = \frac{1}{V}\int_0^{\omega_{cut}} d\omega DOS(\omega)C(\omega)D(\omega) \tag{2}$$

and the AF diffuson contribution is

$$k_{AF} = \frac{1}{V}\sum_{\omega_i>\omega_{cut}} C_i(\omega)D_{AF,i}(\omega) \tag{3}$$

The cut-off frequency ω_{cut} identifies the transition from phonon-like to diffuson modes.[18,19,30] While this transition is not universal for various materials and material properties (see Section), phonon-like behavior can be identified for a-Si and not a-SiO_2 in this work and others, both experimentally[16,21,26,30] and numerically.[18,19,51,54] Identifying the phonon-like behavior for a-Si is not sensitive qualitatively to the choice of model[18,19,30] or ω_{cut}.[18,19,26,30,53]

B. Phonons

For a perfect lattice, all vibrational modes are phonon modes, which by definition are delocalized, propagating plane waves.[55] In an amorphous system, only in the low-frequency, long-wavelength limit are the vibrational modes phonons. In this work, we identify the phonon limit by ω_{cut} in Eq. , which is determined in Section . By identifying ω_{cut} the contribution of phonon-like modes in a-Si and a-SiO_2 is quantified and the thermal conductivity accumulation is predicted in Section .

Using the single-mode relaxation time approximation[55] to solve the Boltzmann transport equation gives Eq. , which is the kinetic theory of a phonon gas.(cite) Further assumed in Eq. are isotropy and a single phonon polarization,(cite) making the properties a function of the mode frequency ω only.

The phonon specific heat $C(\omega)$ is taken to be

$$C(\omega) = \frac{k_{\mathrm{B}}}{V} \tag{4}$$

Because we use molecular dynamics (MD) simulations, we

Since MD simulations are classical and obey Maxwell-Boltzmann statistics,[56] the volumetric specific heat is k_{B}/V per mode in the harmonic limit, where V is the system volume. This harmonic approximation has been shown to be valid for LJ argon and SW silicon at the temperatures of interest here[57,58] and is used so that direct comparisons can be made between the MD- and lattice dynamics-based methods.

In general, the thermal conductivity k_{ph} and group velocity v_g depend on the spatial direction $\mathbf{n}$. Since the amorphous materials studied in this work are isotropic, k_{ph} and v_g are scalar quantities indepdent of the direction $\mathbf{n}$.

The phonon thermal diffusivity, $D(\omega)$, is modeled using

$$D(\omega) = B\omega^{-2} \tag{5}$$

which is a scaling predicted for Umklapp scattering, and

$$D(\omega) = B\omega^{-4} \tag{6}$$

which is the scaling precited by Rayleigh scattering.

In the phonon gas model, the thermal diffusivities can be expressed as

$$D(\omega) = \frac{1}{3}v_g^2(\omega)\tau(\omega) \tag{7}$$

where the physical picture is of propagating plane waves which travel with velocity v_g and for a time τ before scattering. An equivalent physical picture in terms of a scattering length for the thermal diffuivity is

$$D(\omega) = \frac{1}{3}v_g(\omega)\Lambda(\omega), \tag{8}$$

where Λ is the phonon mean free path (MFP), defined as

$$\Lambda(\omega) = v_g(\omega)\tau(\omega). \tag{9}$$

Both defintions Eqs. and are only valid in the propagating limit, i.e. the Ioffe-Regel limit (Eq. or).

Under the Debye approximation, which assumes isotropic and linear dispersion (i.e., $v_g = v_s$), the denisty of states, $DOS(\omega)$, is

$$DOS(\omega) = \frac{3\pi\omega^2}{2v_{s,DOS}^3}, \tag{10}$$

where v_s is an appropriate sound speed (see Section).(cite)

The form for $D(\omega)$ (Eq.) and the $DOS(\omega)$ (Eq.) cause a cancellation of ω dependance in Eq. and ensures the thermal conductivity (Eq.) is finite. The form for $D(\omega)$ (Eq.) causes the thermal conductivity (Eq.) to diverge in the low-frequency limit as the system size is increased as $L^{1/4}$.(cite)

C. Diffusons

For disordered systems, the vibrational modes are no longer pure plane-waves (i.e., phonon modes), except in

the low-frequency (long-wavelength) limit. When applied in the classical limit, the Allen-Feldman (AF) theory computes the contribution of diffusive, non-propagating modes (i.e., diffusons) to thermal conductivity[59]

$$D_{AF,i} = \frac{\pi V^2}{\hbar^2 \omega_i^2} \sum_{j \neq i} |\langle i|J_{x,y,z}|j\rangle|^2 \delta(\omega_i - \omega_j) \quad (11)$$

where $D_{AF,i}$ is the mode diffusivity and ω_i is the frequency of the ith diffuson. The diffusivity of diffusons can be calculated from harmonic lattice dynamics theory.[18,19,59]

D. Thermal Diffusivity Limits

For disordered materials In the low-frequency, long-wavelength limit, the mode thermal diffusivity has the form of Eq. or .(cite) The mode diffusivities generally decrease with increasing frequency,(cite) often reaching a plateau,(cite) and then decrease exponentially to zero as the modes become localized.(cite) The diffuson thermal diffusivities, Eq. , can not, in general, be expressed as either Eq. or , as the mode group velocities, lifetimes, and/or MFPs can not be estimated independently.[18,19,59,60]

It is useful to consider a high-scatter limit for the mode diffusivity,

$$D_{HS} = \frac{1}{3} v_s a, \quad (12)$$

where it is assumed that all vibrational modes travel with the sound speed, v_s, and scatter over a distance of the lattice constant, a. This diffusivity assumption leads to a high-scatter (HS) limit of thermal conductivity in the classical limit[61]

$$k_{HS} = \frac{k_\mathrm{B}}{V_b} b v_s a, \quad (13)$$

where V_b is the volume of the unit cell and b is the number of atoms in the unit cell.

For mode lifetimes which depend on frequency, the Ioffe-Regel (IR) limit is

$$\tau = \frac{2\pi}{\omega}. \quad (14)$$

Assuming linear dispersion ($i.e., \omega = v_s k$), the IR limit for MFP is

$$\Lambda = \lambda, \quad (15)$$

where λ is the wavelength of the vibrational mode. These limits are not equivalent if the group velocity is mode-dependent. Also, it is generally not possible to assign a unique wavenumber to disordered modes.(cite) The IR and HS limits are examined in Section and Section .

For amorphous systems, the spatial disorder creates strong scattering, and k_{vib} tends to be near the high-scatter limit k_{HS}.(cite) It was demonstrated by Kittel that the thermal conductivity of glasses above 20 K could be interpreted using a temperature-independent high-scatter diffusivity on the order of Eq. . Since this corresponds to a phonon model with MFP $\Lambda = a$, too small to justify use of the model, implies that the dominant modes in most glasses are diffusons and not phonons.(cite)

One way to interpret this result is to use assume $k_{vib} = k_{AF} = k_{HS}$. Amorphous Lennard-Jones argon is dominated by high-scatter modes,[62] as is a model of a-GeTe, and both their $k_{vib} \approx k_{HS}$.[52] For a-SiO_2, $k_{vib} \approx 2k_{HS}$, while it is unclear what the appropriate lattice constant a should be.(cite) For a-Si, the thermal conductivity at 300 K $k_{vib} \approx (1-6)k_{HS}$, indicating that there may be a large contribution from k_{ph}.

While Eqs. and are commonly used to establish a high-scatter limit for diffusivity and thermal conductivity, predictions for a-SiGe alloys demonstrated that these are not true high-scatter limits.[18] Recently, the thermal conductivity of several materials has been measured to be significantly below k_{HS}.(cite)

By using lattice dynamics calculations and molecular dynamics simulations, we predict the inputs to Eq. in Section and the thermal conductivity k_{vib} in Section . The MFPs of phonons and diffusons is predicted from Eqs. and , and the thermal conductivity accumulation is predicted in Section

III. CALCULATION DETAILS

A. Sample Preparation

1. *Amorphous Si*

For a-Si, we use models created by the Wooten-Winer-Weaire (WWW) algorithm in Ref. 63. Sample sizes with N_a = 216, 1000, 4096, and 100,000 were provided, where N_a are the number of atoms in the disordered supercell.(cite) A large sample was created from the $N_a = 100,000$ sample by treating it as a unit cell and tiling twice in all directions to create an $N_a = 800,000$ sample with box size L nm. All a-Si structures used have a density ρ equivalent to the perfect crystal with a lattice constant of a =5.43 Å.(cite)

The Stillinger-Weber potential is used with these samples. The samples were annealed at a temperature of 1100 K for 5 ns to remove meta-stability. Amorphous materials have many different atomic (potential energy) configurations with nearly equivalent energies.(cite) The removal of meta-stability is demonstrated by an increase in the predicted sound speeds, $v_{s,T}$ and $v_{S,L}$, after annealing (see Table). This meta-stability can cause errors when predicting vibrational lifetimes using Normal Mode Decomposition (NMD, see Section).(cite)

Similar structures and results can be obtained with a-Si samples created using a melt-quench-anneal procedure,(cite) similar to that used to create a-SiO_2 samples in Section .

(footnote)In an amorhous material, there are many potential energy configurations (atomic positions) which are nearly equivalent in energy. At a sufficient temperature, the meta-stable configurations cause the equillibrium atomic positions to vary in time. This can effect on the prediction of the vibrational mode lifetimes when using the normal mode decomposition method. In the time domain, the average normal mode potential and kinetic energy must be calculated and subtracted from the normal mode energy autocorrelation function.(cite) If the average energy is not specified correctly, unphysically large or small mode lifetimes can be predicted.(cite)

(footnote) The entire procedure is performed at constnat volume. Crystalline silicon (c-Si) is first melted at a temperature of 10,000 K. The liquid is then quenched instantaneously to 300 K, and then annealed at 1100 K for 10 ns to remove meta-stability.

2. *Amorphous SiO_2*

The a-SiO_2 samples are used from Ref. 54 and have size N_a = 288 , 576, and 972. The atomic potentials used for a-SiO_2 are the same as in Ref. 54 except the 24-6 Lennard-Jones potential is changed to a 12-6, which has a negligible effect on the predictions presented in this paper. Larger systems of N_a = 2880, 4608, and 34562 are created by a similar melt-quench technique as that used in Ref. 54

(footnote) The entire procedure is performed at constant volume. Crystalline silicon (c-Si) is first melted at a temperature of 10,000 K. The liquid is then quenched instantaneously to 300 K, and then annealed at 1100 K for 10 ns to remove meta-stability.

B. Simulation Details

Molecular dynamics simulations are performed using the disordered a-SiO_2 and a-Si supercells described in Sections and . The MD simulations were performed using LAMMPS[64] with time steps of dt = 0.00905 , 0.0005 for a-SiO_2 and a-Si. Ten MD simulations with different initial conditions were run for 2^21 time steps and the atomic trajectories sampled ever 2^8 time steps. For the GK method, the thermal conductivity k_{GK} is predicted by window averaging the integral of the heat current autocorrelation function (HCACF).(cite) For a-SiO_2 and s-Si, a interval of the the HCACF integral can be found which is constant within the statistical noise.(cite) Large system sizes up to N_a = 34,000 and 800,000 can be used to predict k_{GK} for a-SiO_2 and a-Si (see Section). For smaller systems, the trajectories from the MD simulations used for the GK method are also used in the NMD method to predict the vibrational mode lifetimes (Section).

For the amorphous supercells studied, the only allowed wave vector is the gamma-point (i.e., $\boldsymbol{\kappa} = 0$), where $\boldsymbol{\kappa}$ is the wavevector and there are $3N_a$ polarization branches labeled by ν. Calculation of the vibrational modes at the Gamma point require the eigenvalue solution of a dynamical matrix of size $(3N_a)^2$ that scales as $[(3N_a)^2]^3$, limiting the system sizes that can be considered to N_a = 4608 and 4096 for a-SiO_2 and a-Si. This eigenvalue solution is also required to perform the NMD (see Section **??**) and AF calculations (see Section IV E). The frequencies and eignvectors were computed using harmonic lattice dynamics calculations and GULP.[65] The calculation of the AF diffuson thermal diffusivities (Eq.) is performed using GULP and a Lorentzian broadening of $5\delta\omega_{avg}$ and $14\delta\omega_{avg}$ for a-Si and a-SiO^2, where $\delta\omega_{avg}$ is the average mode frequency spacing.(cite) Varying the broadening around these values does not change the resulting thermal conductivity k_{AF} significantly (see Section).

IV. VIBRATIONAL PROPERTIES

A. Density of States

In this section, we examine the frequencies and density of states (DOS) for the vibrational modes of a-SiO_2 and a-Si described in Section and . The vibrational DOS is computed by

$$DOS(\omega) = \sum_i \delta(\omega_i - \omega), \tag{16}$$

where a unit step function is used to broaden $\delta(\omega_i - \omega)$.(cite) The DOS for a-$SiO_2$ and a-Si are plotted in Fig. using two values of broadening, $10\delta\omega_{avg}$ and $100\delta\omega_{avg}$. Because of the finite model size, the low-frequency modes are sparse and the DOS has a large variability dependent on the broadening.[19] As the system size L is increased, the lowest frequency mode will continue to decrease and the gaps in frequency will fill in.(cite) The DOS for a-Si is similar to the DOS of crystalline silicon,[53,66] particularly at low-frequency, and with pronounced features as in disordered lattices.[62,67] The DOS for a-SiO_2 is essentially constant over most of the frequency-range, except at the lowest frequencies.

While the DOS has a large amount of variability at low frequency, there is a clear scaling of $DOS \propto \omega^{-2}$ for both a-Si and a-SiO_2. The range of this scaling is larger for a-Si than a-SiO_2. By fitting the DOS from Fig. to Eq. , a sound speed is predicted at reported in Table . For both a-Si and a-SiO_2, the sound speeds predicted from the DOS are close to the transverse sound speeds predicted from the elastic constants and the structure factor. The Debel model (Eq.) predicts that the contribution from the larger longitudinal sound speed compared to the smaller transverse sound speed will scale

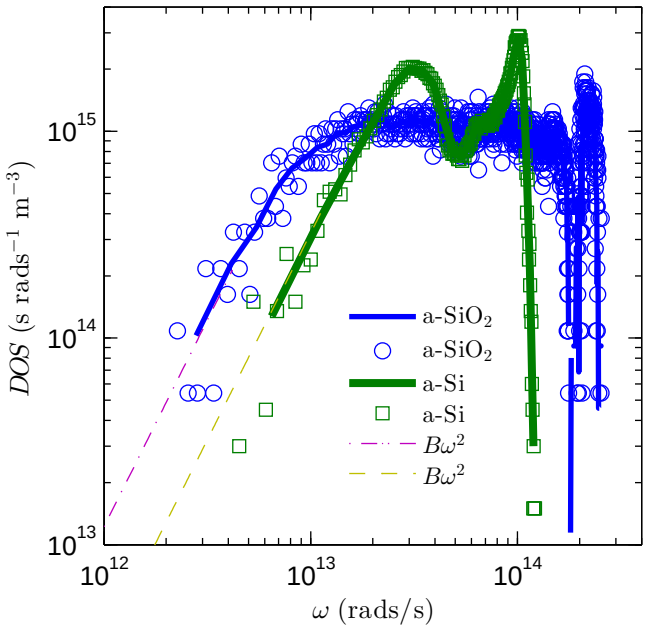

FIG. 1: Vibrational DOS predicted for our models of a-SiO2 and a-Si using Eq. (16). Both models show a scaling at low frequency $DOS(\omega) \propto \omega^{-2}$, which is predicted by the Debye approximation (Eq. (10)) using the transverse sound speeds predicted using various methods (Table I). At high frequency, the DOS of a-SiO2 shows a plateau and then a sharp feature corresponding to a gap in the vibrational spectrum due to the Si and O bonds.(cite) For a-Si, there are two sharp peaks, which show as small peaks in the preditions of the vibrational mode lifetimes (Fig. 3) and mode diffusivities (Fig. 4).

as the difference cubed. For a-Si, the contribution from longitudinal modes to the Debye DOS is nearly an order of magnitude less than the transverse modes for a given frequency interval. For a-SiO_2, the logitudinal and transverse sound speeds are closer.(cite experimental a-DOS)

The intensity for the dynamic structure factor of the TA branch was found to be 6-8 times larger than the LA branch for a model of a-SiO2.[43] A similar factor of 4-5 difference was found in the static structure factors for a mode of a-SiO2.[68] We find that the DOS for our model of a-SiO2 is also dominated by transverse modes (see Table).

The observation that the acoustic modes are located on top of a flat background for intermediate values of q has re- cently been found by G otze and Mayr as an essential result in their analytic calculation of the spectra within mode-coupling theory.[41]

The DOS predicted for jammed systems are similarly dominated by the transverse sound speed,[69] while results for disorded lattices demonstrate[62,67]

B. Group Velocity

For a disordered solid, the three acoustic group velocities (two transverse and one longitudinal) can be predicted using the elastic constants[65] or by finite differencing of the three lowest frequency branches of the dispersion relation of the supercell.[18–20,51,53,62,70] Except for this low-frequency behavior, there is not an accepted method to predict the group velocity of a vibrational mode in a disordered system, although there have been attempts.[20,51,53,61,71] In the Cahill-Pohl (CP) model, for example, the group velocity of all disordered modes is the sound speed, v_s, which is also assumed for the HS model, Eq. (**??**).[61] This assumption is not generally valid for any material.[19,20,51,53,62,71]

Experimentally determined values Freeman gives 4100 m/s for a-SiO_2[9] 3,700 5,100 from[72] for a-Si 3,800-4,800[72] Experimentally measured values of sound speed for a-Si are 4,160[73] and 4,290 m/s[74].[75] For chemical vapor depositioned a-Si thin films, the transverse sound speed is markedly increased $v_{s,T} = 4,740$ m/s.[30]

1. *From Elastic Constants and DOS*

The transverse and logitudinal sound speeds of a material can be related to the material's elastic constants, which determine the bulk (G) and shear (K) moduli.(cite) The transverse sound speed is given by(cite)

$$v_{s,T} = \frac{G}{\rho}^{1/2}, \tag{17}$$

and the longitudinal by

$$v_{s,L} = \frac{4G + 3K}{3\rho}^{1/2}. \tag{18}$$

We use the bulk and shear moduli defined in terms of the elastic constants according to the Voight convention.(cite) The sound speeds calculated from the elastic constants are reported in Table . It is clear that the DOS of our models for a-Si and a-SiO_2 are characterized by using the transverse sound speeds, rather than an averaging of the transverse and longitudinal,

$$v_s = \frac{2}{3}v_{s,L} + \frac{1}{3}v_{s,T}. \tag{19}$$

This is backed up by theoretical(cite) and experimental(cite) results.

2. *From Struture Factor*

Calculating the structure factors of the supercell Gamma modes is a method to test for their plane-wave character at a particular wave vector and polarization corresponding to the VC.[19,76] Feldman et al. used the

structure factor to predict an effective dispersion for a model of amorphous silicon, but did not predict group velocities.[19] Volz and Chen used the dynamic structure factor to predict the dispersion of crystalline SW silicon using MD simulation.[77] Has also been used to determine the dispersion relation from experimentally derived predictions.[78]

The structure factor at a VC wave vector $\boldsymbol{\kappa}_{VC}$ is defined as[76]

$$S^{L,T}(\overset{\boldsymbol{\kappa}}{\omega}) = \sum_{\nu} E^{L,T}(\overset{\boldsymbol{\kappa}}{\nu})\,\delta(\omega - \omega(\overset{\boldsymbol{\kappa}=\mathbf{0}}{\nu})), \tag{20}$$

where the summation is over the Gamma modes, E^T refers to the transverse polarization and is defined as

$$E^{L}(\overset{\boldsymbol{\kappa}}{\nu}) = \left| \sum_{b} \hat{\boldsymbol{\kappa}} \cdot e(\overset{\boldsymbol{\kappa}=\mathbf{0}}{\nu}\ \overset{b}{\alpha}) \exp\left[i\boldsymbol{\kappa} \cdot \boldsymbol{r}_0\left(\overset{l=0}{b}\right)\right] \right|^2 \tag{21}$$

and E^L refers to the longitudinal polarization and is defined as

$$E^{T}(\overset{\boldsymbol{\kappa}}{\nu}) = \left| \sum_{b} \hat{\boldsymbol{\kappa}} \times e(\overset{\boldsymbol{\kappa}=\mathbf{0}}{\nu}\ \overset{b}{\alpha}) \exp\left[i\boldsymbol{\kappa} \cdot \boldsymbol{r}_0\left(\overset{l=0}{b}\right)\right] \right|^2 . \tag{22}$$

In Eqs. (21) and (22), the b summations are over the atoms in the disordered supercell, $\boldsymbol{r}_0\left(\overset{l=0}{b}\right)$ refers to the equilibrium atomic position of atom b in the supercell, l labels the unit cells ($l = 0$ for the supercell), α labels the Cartesian coordinates, and $\hat{\boldsymbol{\kappa}}_{VC}$ is a unit vector. Explicit disorder is included in the Gamma frequencies $\omega(\overset{\boldsymbol{\kappa}=\mathbf{0}}{\nu})$ and the $3N_a$ components of the eigenvectors, $e(\overset{\boldsymbol{\kappa}=\mathbf{0}}{\nu}\ \overset{b}{\alpha})$.

The structure factors $S^{L,T}(\kappa,\omega)$ are plotted in Fig. for a-SiO_2 and a-Si (left and right panels) for wavevectors along the [100] direction of the supercells. The length scale used for the wavevectors, $\kappa = 2\pi/a[100]$, are $a =$ 4.8 and 5.43 $\mathring{A}$ for a-SiO_2 and a-Si, which are based on the atomic number densities.(cite) Frequencies $\omega_0(\kappa)$ and lifetimes $\Gamma(\kappa)$ are predicted by fitting each structure factor peak $S^{L,T}$ to a Lorentzian function

$$S^{L,T}(\overset{\boldsymbol{\kappa}}{\omega}) = \frac{C_0(\boldsymbol{\kappa})}{[\omega_0(\boldsymbol{\kappa}) - \omega]^2 + \Gamma^2(\boldsymbol{\kappa})}, \tag{23}$$

where $C_0(\nu)$ is a constant related to the DOS.[67] A dispersion relation is identified by plotting $\omega_0(\kappa)$ in the middle panel of Fig. , where the bars indicate the peak widths $\Gamma(\kappa)$.

Sound speeds are estimated by finite differencing,

$$v_s = \frac{\delta\omega_0(\kappa)}{\delta\kappa}. \tag{24}$$

Estimates of the sound speeds are found from using finite difference of the peaks in $S_{T,L}$ are shown in Table. The values are close to those obtained from the elastic constants (see Section).

The dispersion for a-SiO_2 For intermediate κ, the longitudinal dispersion for a-SiO_2 more closely resembles the so-called "dispersion law for diffusons", where $\omega \propto q^2$.[67]

TABLE I: Estimated from the elastic constants, the pre-annealed group velocities are $v_{s,T,} = 3,670$, $v_{s,L,elas} = 7,840$ $v_{s,T,elas} = 2,541$, $v_{s,L,elas} = 4,761$ (see Section).

method	Eqs. (17), (18)	Eqs. (20), (24)	DOS Eq. (10)
a-SiO_2			
transverse	3,161	2,732	2,339
longitudinal	5,100	4,779	
a-Si			
transverse	3,886	3,699	3,615
longitudinal	8,271	8,047	

The structure factor gives the frequency spectrum needed to construct a (nonstationary) propagating state with a pure wave vector Q and pure longitudinal or transverse polarization[18]. Only low-frequency vibrations have an (approximate) wavevector in disordered systems, and there is no theorem guranteeing this.[19] you cannot assign a unique wavevector to individual modes, even for low frequency modes.[18,79,80]

Fig 4 of this work shows a dispersion extracted by locating the peaks in the structure factor. The dispersion at low frequency is also dominated by transverse sound speed.[69]

The transverse sound speed predicted by the DOS is used for both a-SiO_2 and a-Si throuhout the rest of this work.

As in other studies we find that there is a positive dispersion of the longitudinal branch initially and then there is the usual negative dis- persion at higher frequencies. The onset of this positive dispersion seems to be approximately as- sociated with the IoffeRegel crossover for trans- verse polarization.[?]

C. Mode Lifetimes

In conclusion, we have found that the high-frequency VS in a realistic model of amorphous Si decay on picosecond time scales, and at low temperatures their lifetimes de- crease as frequency increases. This is in contrast to recent experimental claims that the modes decay on nanosecond scales and their lifetimes increase as frequency increases.[81]

The lifetimes found by this method are in good agreement with the perturbative calculations of Fabian and Allen and are on the order of 10 ps at low tem- peratures in both 216 and 4096 atom supercells.[82]

Our results indicate that all of these processes occur on a much faster time scale than the 1 ns temporal resultion of the Raman experiments, so it is not obvious that the measured relaxation rates should be identified with vibrational lifetimes.[83]

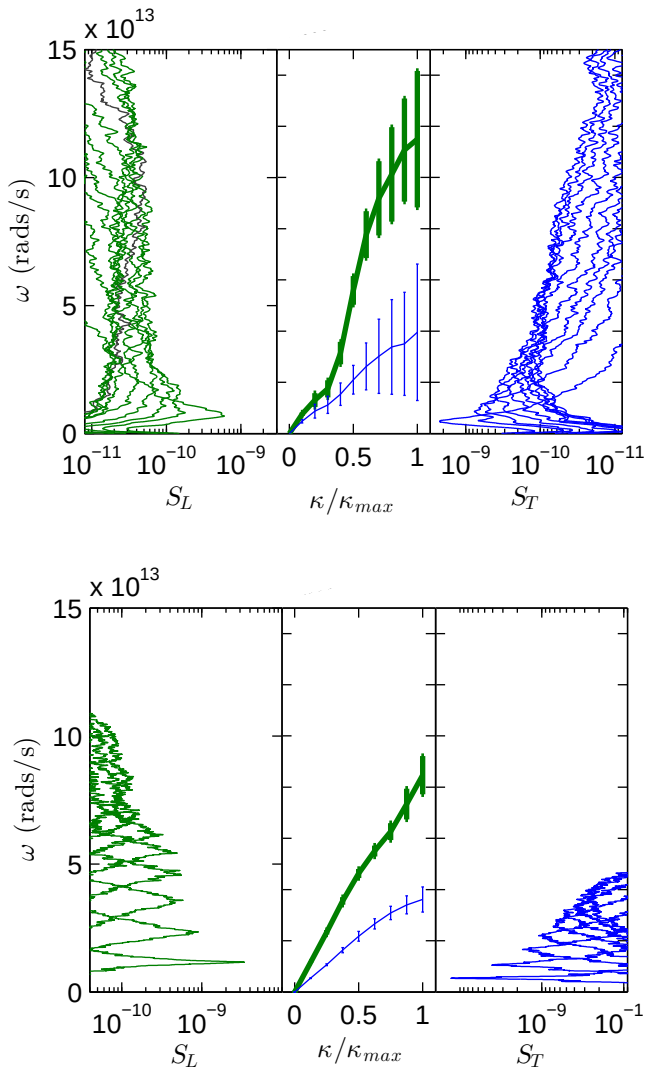

FIG. 2: Longitudinal (left panel) and transverse (right panel) structure factors (Eq. (20)) for a-SiO2 (top plot) and a-Si (bottom plot). Sound speeds are estimated by finite differencing (Eq. (24)) of the lowest frequency peaks and are reported in Table I. The dispersion for a-SiO2 is only linear for the lowest frequency, smallest wavenumbers. The dispersion for a-Si is linear over a wider range of wavenumber. Lifetimes are predicted from the widths of the structure factor peaks (Eq. (23)) and are plotted in Fig. 3.

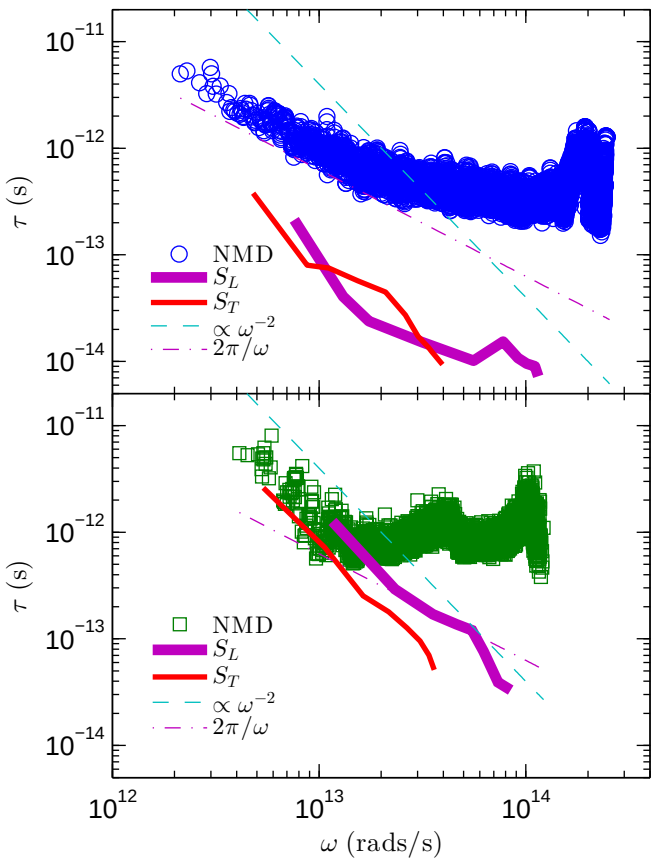

FIG. 3: vibrational mode lifetimes predicted by NMD (Eq.) and the structure factors (Eq.) for a-SiO2 (top plot) and a-Si (bottom plot). The IR limit (Eq.) is a lower limit for the mode lifetimes, while the lifetimes from the structure factors fall below this limit, partiularly for a-SiO2. The structure factor lifetimes generally follow a scaling $\tau \propto \omega^{-2}$ for both systems, while the mode lifetimes show a plateau before crossing the IR limit.

1. *From Structure Factor*

The lifetimes predicted from Eq. are plotted in Fig. for a-SiO2 and a-Si. There is a clear separation for transverse and longitudinal scalings for a-Si with $tau \propto \omega^{-2}$, and the lifetimes are above the IR limit (Eq.) for the lowest frequencies.

For a-SiO2, the separation between transverse and longitudinal is not as clear as in a-Si, and the lifetimes are significantly less than the IR limit, Eq. .

Ioffe-Regel limit[84].

2. *From Normal Mode Decomposition*

We use the MD simulation-based normal mode decomposition (NMD) method to predict the lifetimes of each vibrational mode in the disordered supercells (see Section).[57,85–87] The NMD method can predict vibrational lifetimes which are affected by the disorder in the supercell.(cite)

(footnote) In NMD, the atomic trajectories from MD simulations are first mapped onto the vibrational mode

coordinate time derivative,[88]

$$\dot{q}(\boldsymbol{\kappa}_{\nu}^{=\mathbf{0}};t) = \sum_{\alpha,b,l}^{3,n,N} \sqrt{\frac{m_b}{N}} \dot{u}_{\alpha}(\begin{smallmatrix} l \\ b \end{smallmatrix};t)\, e^{*}(\boldsymbol{\kappa}_{\nu}^{=\mathbf{0}}\ \begin{smallmatrix} b \\ \alpha \end{smallmatrix}) \exp[i(\mathbf{0}\cdot\mathbf{r}_0(\begin{smallmatrix} l \\ 0 \end{smallmatrix})]. \tag{25}$$

Here, m_b is the mass of the b_{th} atom in the unit cell, u_α is the α-component of the atomic displacement from equilibrium, $\dot{u}_\alpha$ is the α-component of the atomic velocity, and t is time. The spectral energy of each vibrational mode, $\Phi(\boldsymbol{\kappa}_{\nu};t)$, is calculated from

$$\Phi(\nu,\omega) = \lim_{\tau_0\to\infty} \frac{1}{2\tau_0} \left| \frac{1}{\sqrt{2\pi}} \int_0^{\tau_0} \dot{q}(\boldsymbol{\kappa}_{\nu}^{=\mathbf{0}};t) \exp(-i\omega t) dt \right|^2, \tag{26}$$

The vibrational mode frequency and lifetime is predicted by fitting each mode's spectral energy $\Phi(\nu,\omega)$ (see Appendix) to a Lorentzian function

$$\Phi(\nu,\omega) = \frac{C_0(\nu)}{[\omega_0(\nu)-\omega]^2 + \Gamma^2(\nu)}, \tag{27}$$

where the constant $C_0(\nu)$ is related to the average energy of each mode and the linewidth $\Gamma(\nu)$.[87] The mode lifetime is given by

$$\tau(\nu) = \frac{1}{2\Gamma(\nu)} \tag{28}$$

For a-SiO2, the mode lifetimes are generally larger than the IR limit Eq. , and follow this limit at low frequency. At high frequency the mode lifetimes are roughly constant without definite scaling. There is a peak near 2 $10^{14} rads/s which correspondstoapeakintheDOS(seeFig.)$.

The mode lifetimes show a similar plateau at higher frequencies, particularly for a-Si, which has been reported for disordered lattices.[62]

For a-Si, a transition to a constant lifetime plateau occurs near 1 $10^{14} rads/s, whichcorrespondstowheretheDOSpeaksinFig.$ Similar behavior was found for disordered lattices.[51,62]

3. Discussion

For model a-LJ, the lifetimes predicted by the static and dynamic structure factors and the NMD method are in close agreement at low temperature.[89] At low frequency for our model of a-Si, good agreement sis found between the structure factor and NMD predicted lifetimes.

The lifetimes predicted by NMD and scaled by the sound speed diverge from the AF predicted mode diffusivities when the mode lifetimes approach the IR limit, shown in Fig. . This is an indication that the modes have transitioned from propagating (where the diffusivity D and lifetime are related by $D = (1/3)v_s^2\tau$) to non-propagating where D and τ need not be related.[18,19,59,60]

For a model of a-SiO2, the lowest frequency structure factor lifetimes (inverse linewidths) are already below the IR limit.[68]

These time scales are close to those reported in Ref for similar a-Si structures. The lifetimes are also on the order of those reported for similar models of a-Si using MD-based and anharmonic lattice dynamics methods.(cite)

Fabian finds lifetimes on the order of picoseconds for a-Si and para-crystalline silicon.[81,90]

A previous study of a-Si predicted vibrational lifetimes on the order of 100 ps, about ten times the values reported here and in other studies.(cite) While the samples

For a-Si, the scaling at low frequency shows $\tau \propto \omega^{-2}$. The same scaling was found in previous studies using similar models for a-Si.(cite)

Also shown as a solid curve is the phonon gas model, where the fitted formula 1/ Q 2 i Q 2 is used for transverse i propagons, and it is assumed that transverse and longitudinal propagons have the same diffusivity. Notice that the gas- model result fits perfectly onto the higher frequency diffuson result, indicating mutual consistency of the two different transport theories in the region of overlap 10 meV 20 meV.

A numerical investigation of Bickham[83] indeed shows that a strong perturbation of the vibrational spectrum of a-Si can relax on a 100 ps time scale, compared to 10 ps for a weak perturbation. In addition to pure vibra- tional relaxation, it is also likely, as suggested by Bickham and Feldman,[82] that correspondingly large local deviations in the atomic displacements cause local structural rearrange- ments which may relax to local metastable minima while emitting phonons.

D. Diffusivities

Thermal diffusivity was predicted for a percolation network which showed Rayleigh type scattering dependance in the low-frequency limit.[91]

which generally agree with diffusivities computed according to the formula of Edwards and Thouless.[92]

Thermal diffusivity has been predicted using a wave-packet method

It was shown

Garber shows that these high-frequency modes are localized in the Anderson sense, showing exponential decay of the mode eigenvector.[93]

It was shown that the diffusivity $D_{AF}(\omega) \propto DOS(\omega)$ at low frequency when the modes are spatially uncorrelated and the overlap between them is small and independent of the frequency.[69,94]

At low frequencies, the AF-predicted and NMD-predicted mode diffusivities scale as $D \propto \omega^{-2}$, similar to the scaling due to Umklapp scattering of phonons in a crystalline system. Rayleigh scattering due to point defects predicts $D \propto \omega^{-4}$, but is not observed in the amorphous systems studied in this work.(cite) While Rayleigh-type scaling has been observed in harmonic studies of the

diffusivities of modes in disordered lattics and jammed systems,[69,91,94] it has been demonstrated that the harmonic disorder in a-Si produces a scaling similar to Umklapp scattering.[18]

In summary, we obtain a frequency-independent diffusiv- ity when the density of states is frequency-independent and the following conditions are satisfied: A displacements of particles in different modes of similar frequency are uncor- related; B the directions of changes in the relative displace- ments of pairs of interacting particles are spatially uncorre- lated within a given mode; and C the direction of change in the relative displacement of a pair of interacting particles is uncorrelated from the direction of the displacement.

Both a-SiO_2 and a-Si have a region at higher frequencies where the AF-predicted mode diffusivities are relatively constant. This behavior has been reported for a number of disordered systems such as disordered lattices[62,67,91] and jammed systems. At the higest frequencies the AF-predicted diffusivities trend exponentially to zero, which is an indication that these modes are "locons", spatially localized modes which do not contribute to thermal condutivity.[76]

This perplexing property of glasses has been explained heuristically by assuming that phonons are scattered so strongly by structural disorder that trans- port becomes diffusive, with a frequency regime of small, constant thermal diffusivity.[59,91,95]

E. Discussion

This supports the idea of Slack for a-SiO_2[96] While the thermal conductivity of a-SiO , the material is characterized by a constant similar for other amorphous materials such as Lennard-Jones argon[62] and a model of a-GeTe.[52]

At low frequency, our model supports the scaling $D(\omega) = B\omega^{-2}$ and not $D(\omega) = B\omega^{-4}$ as is predicted by the Rayleigh scattering from density fluctuations acting as scattering centers.(cite) Rayleigh scattering

Using the NMD-predicted lifetimes and AF-predicted diffusivities, a representative velocity can be computed,

$$v_{AF}(\omega) = \left(3\frac{D_{AF,i}(\omega)}{\tau(\omega)}\right)^{1/2}, \tag{29}$$

and is shown in the inset of Fig. . For a-Si, v_{AF} follows a decreasing trend with increasing frequency, similar to the trend for group velocities in a simple monatomic crystal.(cite)

F. Mean Free Paths

Using the lifetimes predicted from the structure factor peaks and the transverse sound speed, the MFP is about the size of the simulation cell L.

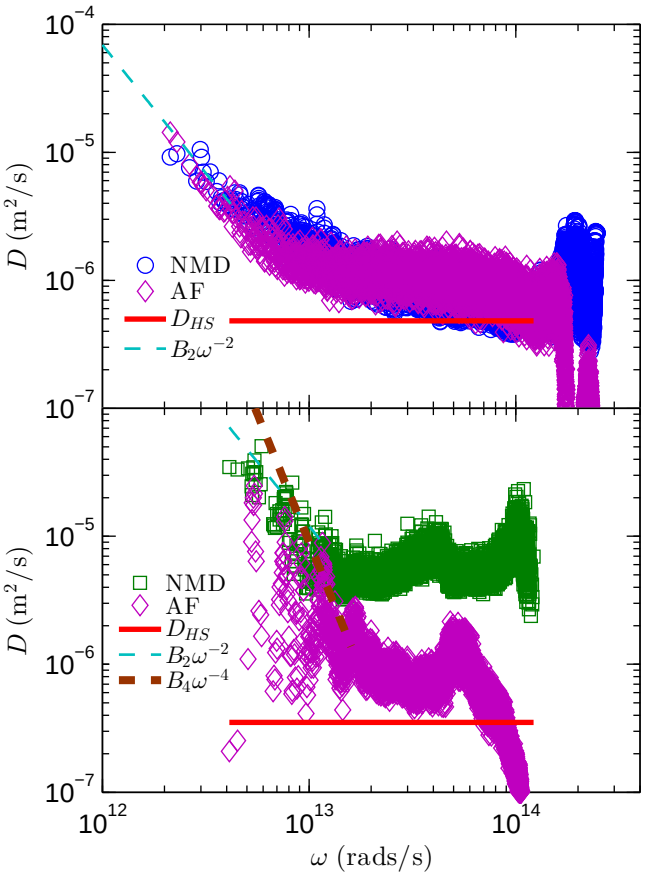

FIG. 4: vibrational mode diffusivities predicted from NMD (using Eqs. (7) and (28) with the sound speed $v_{s,DOS}$ from Table I) and AF theory (Eq. (11)). Also shown are the extrapolations Eqs. (5) and (6), which are used with Eq. (2) to predict the thermal conductivity accumulations in Fig. , and the high-scatter limit Eq. (12).

$$\Lambda_{AF}(\omega) = (3D_{AF,i}(\omega)\tau(\omega))^{1/2}, \tag{30}$$

V. THERMAL CONDUCTIVITY

A. Bulk

Lee found a value of around 1 W/m-K but with very small supercell sizes.[97]

We use the GK method to predict the thermal conductivity. The GK method is relatively inexpensive compared to the NMD and AF methods so that large system sizes can be simulated (see Section).

For smaller system sizes, the same trajectories are used for the GK and NMD methods. The MD simulations

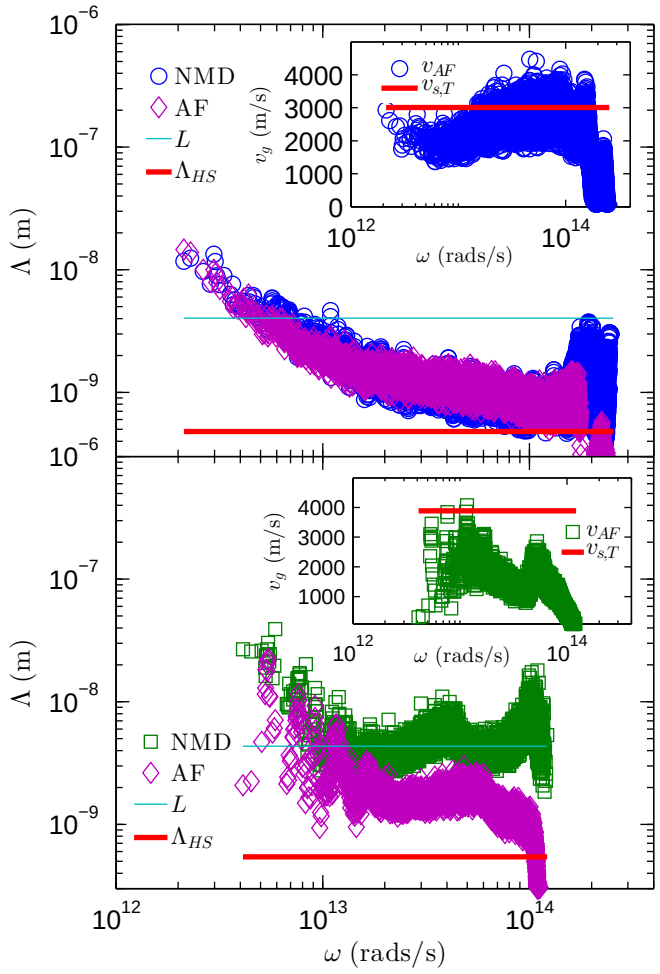

FIG. 5: vibrational MFPs predicted from NMD using Eq. (9) and the sound speed predicted in Table I and from NMD and AF using Eq. (30). Good agreement between the two methods is seen at low frequency, indicating that the modes are propagating and Eqs. (7) and (8) are valid. The majority of MFPs in the intermediate the high-frequency range lie between the simulation box size L and the bond distance a. The inset compares the representative mode velocities Eq. (29) and the sound speeds. For a-Si, v_{AF} decreases with increasing freuquency, similar to the behavior of a monatomic crystal.(cite) The MFPs and mode velocities only approach zero at the highest frequencies, which is an indication that the modes are localized.

were run with the same parameters as the NMD metho (see Section).

The predicted thermal condcutivties from the GK method are plotted in Fig. . For a-SiO2, the thermal conductivity is size independent within the errors. For a-Si, there is a clear size-dependance of the thermal conductivity

To compare the results of the mode-based methods (NMD and AF) and the GK method, it is necessary to es-

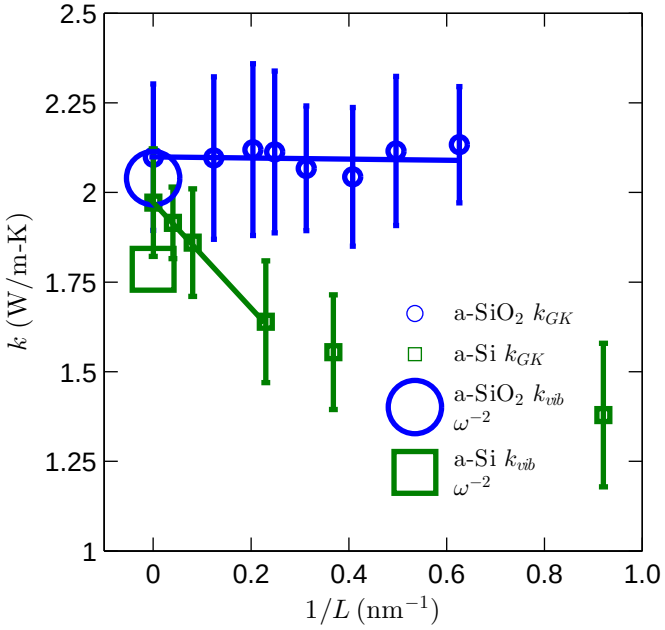

timate the missing contribution from vibrational modes with frequency less than the minimum frequency of the finnite systems.

Assuming the thermal conductivity form Eq. for the lowest frequency modes in the system, the thermal conductivity as a function of the system size takes the form

$$\frac{k(L)}{k_{bulk}} = 1 - \frac{c_0}{L}, \tag{31}$$

"We find that we cannot define a wave vector for the majority of the states, but the intrinsic harmonic diffusivity is still well-defined and has a numerical value similar to what one gets by using the Boltzmann result, replacing v by a sound velocity and replacing l by an interatomic distance a. "[18]

"In order to fit the experimental sc(T) it is necessary to add a Debye- like continuation from 10 meV down to 0 meV. The harmonic diffusivity becomes a Rayleigh m law and gives a divergent (T) as T O. To eliminate this we make the standard assumption of resonant- plus-relaxational absorption from two-level systems (this is an anharmonic effect which would lie outside our model even if it did contain two-level systems implicitly). "[18]

Debye model. $k_tot = k_phonon + k_AF.Forlackofarigorousdefinitionofphononvsdiffusion, wewilld$ $k_debye.$

The relative contribution of $k_phononandk_AFisalsopredictedtobesimilarforsiliconnanowires.$[53]

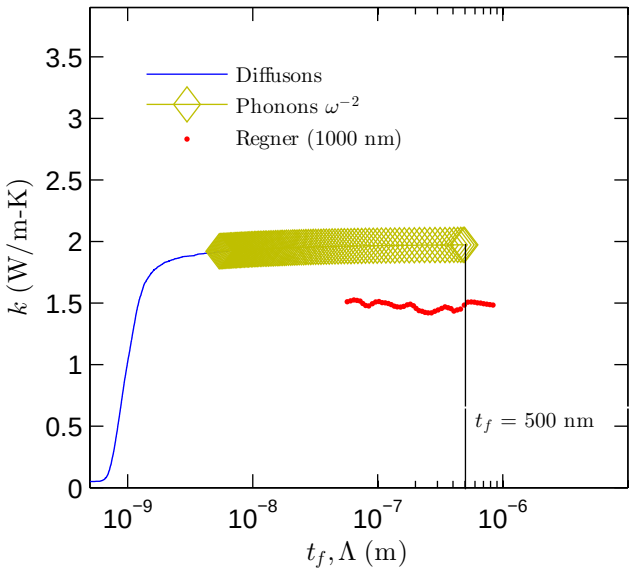

FIG. 7: Thermal conductivity accumulations and thermal conducitivities versus film thickness for a-SiO2 (top plot) and a-Si (bottom plot) from: (i) predictions from this work, (ii) recent broadband measurements of Regner et al, (iii) various experimental measurements for a wide-range of a-Si film thicknesses. While the thermal conductivity predictions for a-SiO2 and a-Si in this work seem to be well-characterized by Umklapp type scaling of the MFPs (Eq. (5)), this scaling is not able to predict the dramatic increase of thermal conducitivity with increasing film thickness from experimentl measurements of a-Si thin films.

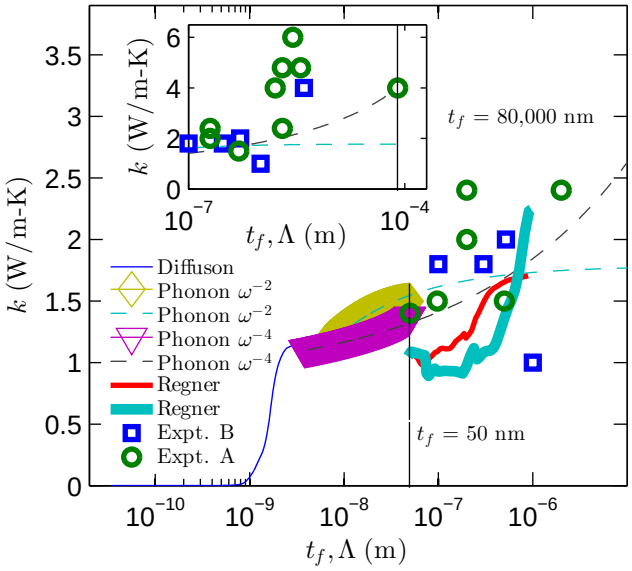

FIG. 8: film thickness dependant thermal conductivity of a-Si from experiment.

B. Accumulation

$$\frac{1}{\Lambda_{eff}(\omega)} = \frac{1}{\Lambda(\omega)} + \frac{1}{t_f}, \tag{32}$$

C. Discussion

Amorphous silicon, however, can be prepared only in thin films, where voids and other inho- mogeneities are unavoidable. Voids loosen the strict re- quirements of a tetrahedral random network (for example, by introducing free boundary conditions). The broadband experiments must then be performed on films prepared using the same technique over a wider-range of film thicknesses (1-100 microns). (cite)

This agress with previous estimates for the contribution of low frequency ($\omega < 30 rads/s$)[98]

Moedling shows that alloying a-Si with Ge can further reduce the thermal conductivity of the bulk and thin films.[18,99]

scattering from static imperfections would predicts Rayleigh type scattering[100] what if you choose a rayleigh type model with "To implement Eq. 6 one must know the correct Q dependence of Q . As shown in Fig. 8, the fitted values scatter too much to guide the extrapolation well. In principle, at very small Q one should get a form Q CQ 4 which corresponds to Rayleigh scattering of sound waves from the structural disorder. The data of Fig. 8 do not fit a Q 4 law; the Q 2 curve shown in the figure is a better fit. Two experiments13,15 but not a third35 and one calculation18 on a-SiO2 have also given Q 2 . We do not know a theory which can give this law in a harmonic model.

The agree- ment between the 3! and the TDTR measurements at 1.11 MHz suggests that phonons with ¿ D=!1=2 14 612 nm are not significant for thermal conduction in this sample. Furthermore, the difference between the high and low frequency measurements by TDTR indicates that pho- nons with 162 ¡ ¡ 612 nm contribute 40% of the of the sample.[30]

The acoustic projected spectral density SQ; E is shown in Fig. 3. From the Q 14 h100i transverse and longitudinal projections, we obtain the respective phase velocities of vt = 4,740 v_l = 7,830 m/s Wooten model, where v_t is significantly higher than the value for our a-Si model (see Table).[30]

Even though the DOS of the WWW produced structures compare well with other models and also experimental measurements, it has been demonstrated that the spectral properties at low frequency can be much different, particularly the linewdith of the structure factor.[30] It is possible that the

Based on the variation of thermal conductivity with film thickness, Liu et al also report a MFP scaling of $\Lambda \propto \omega^{-2}$.[30]

Tight-binding models for a-Si can improve the low-frequency DOS prediction compared to experiment.[101]

A combination of frequency-domain, time-domain, and variable physical heating size measurments would be helpful in investigating[14,16,21,102]

VI. SUMMARY

Table **??**.

[1] D. G. Cahill, W. K. Ford, K. E. Goodson, G. D. Mahan, A. Majumdar, H. J. Maris, R. Merlin, and S. R. Phillpot, Journal of Applied Physics **93**, 793818 (2003).

[2] J.-K. Yu, S. Mitrovic, D. Tham, J. Varghese, and J. R. Heath, Nature Nanotechnology **5**, 718721 (2010).

[3] A. I. Hochbaum, R. Chen, R. D. Delgado, W. Liang, E. C. Garnett, M. Najarian, A. Majumdar, and P. Yang, Nature **451**, 163167 (2008).

[4] G. Pernot, M. Stoffel, I. Savic, F. Pezzoli, P. Chen, G. Savelli, A. Jacquot, J. Schumann, U. Denker, I. Mnch, et al., Nat Mater **9**, 491 (2010), ISSN 1476-1122, URL http://dx.doi.org/10.1038/nmat2752.

[5] A. I. Boukai, Y. Bunimovich, J. Tahi-Kheli, J.-K. Yu, W. A. G. Goddard, and J. R. Heath, Nature **451**, 168171 (2008).

[6] B. Poudel, Q. Hao, Y. Ma, Y. Lan, A. Minnich, B. Yu, X. Yan, D. Wang, A. Muto, D. Vashaee, et al., Science **320**, 634638 (2008), URL http://www.sciencemag.org/content/320/5876/634.abstract.

[7] A. Ward and D. A. Broido, Phys. Rev. B **81**, 085205 (2010), URL http://link.aps.org/doi/10.1103/PhysRevB.81.085205.

[8] M. G. Holland, Physical Review **132**, 2461 (1963).

[9] J. J. Freeman and A. C. Anderson, Physical Review B **34**, 5684\textbackslashtextbackslashtextbackslash965690 (1986).

[10] D. G. Cahill, S. K. Watson, and R. O. Pohl, Phys. Rev. B **46**, 61316140 (1992), URL http://link.aps.org/doi/10.1103/PhysRevB.46.6131.

[11] G. D. Mahan and F. Claro, Phys. Rev. B **38**, 19631969 (1988), URL http://link.aps.org/doi/10.1103/PhysRevB.38.1963.

[12] G. Chen, Journal of Nanoparticle Research **2**, 199 (2000), ISSN 1388-0764, URL http://dx.doi.org/10.1023/A%3A1010003718481.

[13] A. D. Christianson, M. D. Lumsden, O. Delaire, M. B. Stone, D. L. Abernathy, M. A. McGuire, A. S. Sefat, R. Jin, B. C. Sales, D. Mandrus, et al., Phys. Rev. Lett. **101**, 157004 (2008), URL http://link.aps.org/doi/10.1103/PhysRevLett.101.157004.

[14] Y. K. Koh and D. G. Cahill, Phys. Rev. B **76**, 075207 (2007), URL http://link.aps.org/doi/10.1103/PhysRevB.76.075207.

[15] M. Highland, B. C. Gundrum, Y. K. Koh, R. S. Averback, D. G. Cahill, V. C. Elarde, J. J. Coleman, D. A. Walko, and E. C. Landahl, Phys. Rev. B **76**, 075337 (2007), URL http://link.aps.org/doi/10.1103/PhysRevB.76.075337.

[16] A. J. Minnich, J. A. Johnson, A. J. Schmidt, K. Esfarjani, M. S. Dresselhaus, K. A. Nelson, and G. Chen, Phys. Rev. Lett. **107**, 095901 (2011), URL http://link.aps.org/doi/10.1103/PhysRevLett.107.095901.

[17] F. Yang and C. Dames, Physical Review B **87**, 035437 (2013), URL http://link.aps.org/doi/10.1103/PhysRevB.87.035437.

[18] J. L. Feldman, M. D. Kluge, P. B. Allen, and F. Wooten, Physical Review B **48**, 1258912602 (1993).

[19] J. L. Feldman, P. B. Allen, and S. R. Bickham, Phys. Rev. B **59**, 35513559 (1999), URL http://link.aps.org/doi/10.1103/PhysRevB.59.3551.

[20] Y. He, D. Donadio, J.-H. Lee, J. C. Grossman, and G. Galli, ACS Nano **5**, 1839\textbackslashtextbackslashtextbackslashtextbackslashtextbackslashtextbackslash (2011).

[21] K. T. Regner, D. P. Sellan, Z. Su, C. H. Amon, A. J. McGaughey, and J. A. Malen, Nat Commun **4**, 1640 (2013), URL http://dx.doi.org/10.1038/ncomms2630.

[22] S.-M. Lee and D. G. Cahill, Journal of Applied Physics **81**, 25902595 (1997).

[23] T. Yamane, N. Nagai, S.-i. Katayama, and M. Todoki, Journal of Applied Physics **91**, 97729776 (2002), URL http://link.aip.org/link/?JAP/91/9772/1.

[24] H. Wada and T. Kamijoh, Japanese Journal of Applied Physics **35**, L648L650 (1996), URL http://jjap.jsap.jp/link?JJAP/35/L648/.

[25] B. L. Zink, R. Pietri, and F. Hellman, Physical Review Letters **96**, 055902 (2006), URL http://link.aps.org/doi/10.1103/PhysRevLett.96.055902.

[26] H.-S. Yang, D. G. Cahill, X. Liu, J. L. Feldman, R. S. Crandall, B. A. Sperling, and J. R. Abelson, Phys. Rev. B **81**, 104203 (2010), URL http://link.aps.org/doi/10.1103/PhysRevB.81.104203.

[27] D. G. Cahill, M. Katiyar, and J. R. Abelson, Physical Review B **50**, 60776081 (1994).

[28] B. S. W. Kuo, J. C. M. Li, and A. W. Schmid, Applied Physics A: Materials Science & Processing **55**, 289296 (1992), ISSN 0947-8396, 10.1007/BF00348399, URL http://dx.doi.org/10.1007/BF00348399.

[29] S. Moon, M. Hatano, M. Lee, and C. P. Grigoropoulos, International Journal of Heat and Mass Transfer **45**, 2439 2447 (2002), ISSN 0017-9310, URL http://www.sciencedirect.com/science/article/pii/S0017931001003477.

[30] X. Liu, J. L. Feldman, D. G. Cahill, R. S. Crandall, N. Bernstein, D. M. Photiadis, M. J. Mehl, and D. A. Papaconstantopoulos, Phys. Rev. Lett. **102**, 035901 (2009), URL http://link.aps.org/doi/10.1103/PhysRevLett.102.035901.

[31] L. Wieczorek, H. Goldsmid, and G. Paul, in *Thermal Conductivity 20*, edited by D. Hasselman and J. Thomas, J.R. (Springer US, 1989), pp. 235–241, ISBN 978-1-4612-8069-9, URL http://dx.doi.org/10.1007/978-1-4613-0761-7_22.

[32] R. C. Zeller and R. O. Pohl, Phys. Rev. B **4**, 20292041 (1971), URL http://link.aps.org/doi/10.1103/PhysRevB.4.2029.

[33] J. E. Graebner, B. Golding, and L. C. Allen, Phys. Rev. B **34**, 56965701 (1986), URL http://link.aps.org/doi/10.1103/PhysRevB.34.5696.

[34] A. Wischnewski, U. Buchenau, A. J. Dianoux, W. A. Kamitakahara, and J. L. Zarestky, Phys. Rev. B **57**, 26632666 (1998), URL http://link.aps.org/doi/10.1103/PhysRevB.57.2663.

[35] C. Masciovecchio, G. Baldi, S. Caponi, L. Comez, S. Di Fonzo, D. Fioretto, A. Fontana, A. Gessini, S. C. Santucci, F. Sette, et al., Phys. Rev. Lett. **97**, 035501 (2006), URL http://link.aps.org/doi/10.1103/PhysRevLett.97.035501.

[36] W. Schirmacher, EPL (Europhysics Letters) **73**, 892 (2006), URL http://stacks.iop.org/0295-5075/73/i=6/a=892.

[37] W. Schirmacher, G. Ruocco, and T. Scopigno, Phys. Rev.

Lett. **98**, 025501 (2007), URL http://link.aps.org/doi/10.1103/PhysRevLett.98.025501.

[38] B. Ruffl, M. Foret, E. Courtens, R. Vacher, and G. Monaco, Phys. Rev. Lett. **90**, 095502 (2003), URL http://link.aps.org/doi/10.1103/PhysRevLett.90.095502.

[39] M. Wyart, EPL (Europhysics Letters) **89**, 64001 (2010), URL http://stacks.iop.org/0295-5075/89/i=6/a=64001.

[40] J. Fabian and P. B. Allen, Phys. Rev. Lett. **82**, 14781481 (1999), URL http://link.aps.org/doi/10.1103/PhysRevLett.82.1478.

[41] W. Gtze and M. R. Mayr, Phys. Rev. E **61**, 587606 (2000), URL http://link.aps.org/doi/10.1103/PhysRevE.61.587.

[42] H. Shintani and H. Tanaka, Nat Mater **7**, 870 (2008), ISSN 1476-1122, URL http://dx.doi.org/10.1038/nmat2293.

[43] J. Horbach, W. Kob, and K. Binder, The European Physical Journal B - Condensed Matter and Complex Systems **19**, 531 (2001), ISSN 1434-6028, URL http://dx.doi.org/10.1007/s100510170299.

[44] G. Ruocco and F. Sette, Journal of Physics: Condensed Matter **13**, 9141 (2001), URL http://stacks.iop.org/0953-8984/13/i=41/a=307.

[45] P. Benassi, M. Krisch, C. Masciovecchio, V. Mazzacurati, G. Monaco, G. Ruocco, F. Sette, and R. Verbeni, Phys. Rev. Lett. **77**, 38353838 (1996), URL http://link.aps.org/doi/10.1103/PhysRevLett.77.3835.

[46] J. K. Christie, S. N. Taraskin, and S. R. Elliott, Journal of Non-Crystalline Solids **353**, 2272 (2007), ISSN 0022-3093, URL http://www.sciencedirect.com/science/article/pii/S0022309307002840.

[47] W. Schirmacher, G. Diezemann, and C. Ganter, Phys. Rev. Lett. **81**, 136139 (1998), URL http://link.aps.org/doi/10.1103/PhysRevLett.81.136.

[48] S. N. Taraskin, Y. L. Loh, G. Natarajan, and S. R. Elliott, Phys. Rev. Lett. **86**, 12551258 (2001), URL http://link.aps.org/doi/10.1103/PhysRevLett.86.1255.

[49] V. Martin-Mayor, M. Mezard, G. Parisi, and P. Verrocchio, The Journal of Chemical Physics **114**, 8068 (2001), URL http://link.aip.org/link/?JCP/114/8068/1.

[50] S. Ciliberti, T. S. Grigera, V. Martin-Mayor, G. Parisi, and P. Verrocchio, The Journal of Chemical Physics **119**, 8577 (2003), URL http://link.aip.org/link/?JCP/119/8577/1.

[51] Y. He, D. Donadio, and G. Galli, Applied Physics Letters **98**, 144101 (2011), URL http://link.aip.org/link/?APL/98/144101/1.

[52] G. C. Sosso, D. Donadio, S. Caravati, J. Behler, and M. Bernasconi, Phys. Rev. B **86**, 104301 (2012), URL http://link.aps.org/doi/10.1103/PhysRevB.86.104301.

[53] D. Donadio and G. Galli, Phys. Rev. Lett. **102**, 195901 (2009).

[54] A. J. H. McGaughey and M. Kaviany, International Journal of Heat and Mass Transfer **47**, 17831798 (2004).

[55] J. M. Ziman, *Electrons and Phonons* (Oxford, New York, 2001).

[56] D. A. McQuarrie, *Statistical Mechanics* (University Science Books, Sausalito, 2000).

[57] A. J. H. McGaughey and M. Kaviany, Physical Review B **69**, 094303 (2004).

[58] J. V. Goicochea, M. Madrid, and C. H. Amon, Journal of Heat Transfer **132**, 012401 (2010).

[59] P. B. Allen and J. L. Feldman, Physical Review B **48**, 1258112588 (1993).

[60] P. B. Allen and J. Kelner, American Journal of Physics **66**, 497506 (1998).

[61] D. Cahill and R. Pohl, Annual Review of Physical Chemistry **39**, 93121 (1988).

[62] J. Larkin and A. McGaughey, Journal of Applied Physics (2013).

[63] G. T. Barkema and N. Mousseau, Phys. Rev. B **62**, 49854990 (2000), URL http://link.aps.org/doi/10.1103/PhysRevB.62.4985.

[64] S. Plimpton, Journal of Computational Physics **117**, 1 19 (1995), ISSN 0021-9991, URL http://www.sciencedirect.com/science/article/pii/S002199918571039X.

[65] J. D. Gale and A. L. Rohl, Molecular Simulation **29**, 291 (2003).

[66] M. L. Williams and H. J. Maris, Phys. Rev. B **31**, 45084515 (1985), URL http://link.aps.org/doi/10.1103/PhysRevB.31.4508.

[67] Y. M. Beltukov, V. I. Kozub, and D. A. Parshin, Phys. Rev. B **87**, 134203 (2013), URL http://link.aps.org/doi/10.1103/PhysRevB.87.134203.

[68] S. N. Taraskin and S. R. Elliott, EPL (Europhysics Letters) **39**, 37 (1997), URL http://stacks.iop.org/0295-5075/39/i=1/a=037.

[69] V. Vitelli, N. Xu, M. Wyart, A. J. Liu, and S. R. Nagel, Phys. Rev. E **81**, 021301 (2010), URL http://link.aps.org/doi/10.1103/PhysRevE.81.021301.

[70] T. Hori, T. Shiga, and J. Shiomi, Journal of Applied Physics **113**, 203514 (2013), URL http://link.aip.org/link/?JAP/113/203514/1.

[71] J. C. Duda, T. S. English, D. A. Jordan, P. M. Norris, and W. A. Soffa, Journal of Physics: Condensed Matter **23**, 205401 (2011), URL http://stacks.iop.org/0953-8984/23/i=20/a=205401.

[72] R. O. Pohl, X. Liu, and E. Thompson, Rev. Mod. Phys. **74**, 9911013 (2002), URL http://link.aps.org/doi/10.1103/RevModPhys.74.991.

[73] W. Senn, G. Winterling, M. Grimsditch, and M. Brodsky, in *Inst. Phys. Conf. Ser* (1979), p. 709.

[74] R. Vacher, H. Sussner, and M. Schmidt, Solid State Communications **34**, 279 (1980), ISSN 0038-1098, URL http://www.sciencedirect.com/science/article/pii/0038109880905578.

[75] J. L. Feldman, J. Q. Broughton, and F. Wooten, Phys. Rev. B **43**, 21522158 (1991), URL http://link.aps.org/doi/10.1103/PhysRevB.43.2152.

[76] P. B. Allen, J. L. Feldman, J. Fabian, and F. Wooten, Philosophical Magazine B **79**, 17151731 (1999).

[77] S. Volz and G. Chen, Physical Review B **61**, 26512656 (2000).

[78] N. L. Green, D. Kaya, C. E. Maloney, and M. F. Islam, Physical Review E **83**, 051404 (2011), URL http://link.aps.org/doi/10.1103/PhysRevE.83.051404.

[79] R. Biswas, A. M. Bouchard, W. A. Kamitakahara, G. S. Grest, and C. M. Soukoulis, Phys. Rev. Lett. **60**, 22802283 (1988), URL http://link.aps.org/doi/10.1103/PhysRevLett.60.2280.

[80] L. E. Silbert, A. J. Liu, and S. R. Nagel, Phys. Rev. E **79**, 021308 (2009), URL http://link.aps.org/doi/10.1103/PhysRevE.79.021308.

[81] J. Fabian and P. B. Allen, Phys. Rev. Lett. **77**,

38393842 (1996), URL http://link.aps.org/doi/10.1103/PhysRevLett.77.3839.

[82] S. R. Bickham and J. L. Feldman, Phys. Rev. B **57**, 1223412238 (1998), URL http://link.aps.org/doi/10.1103/PhysRevB.57.12234.

[83] S. R. Bickham, Phys. Rev. B **59**, 48944897 (1999), URL http://link.aps.org/doi/10.1103/PhysRevB.59.4894.

[84] S. N. Taraskin and S. R. Elliott, Philosophical Magazine Part B **79**, 17471754 (1999), URL http://www.tandfonline.com/doi/abs/10.1080/13642819908223057.

[85] A. J. C. Ladd, B. Moran, and W. G. Hoover, Physical Review B **34**, 50585064 (1986).

[86] J. E. Turney, E. S. Landry, A. J. H. McGaughey, and C. H. Amon, Phys. Rev. B **79**, 064301 (2009), URL http://link.aps.org/doi/10.1103/PhysRevB.79.064301.

[87] J. M. Larkin, J. E. Turney, A. D. Massicotte, C. H. Amon, and A. J. H. McGaughey, to appear in Journal of Computational and Theoretical Nanoscience (2012).

[88] M. T. Dove, *Introduction to Lattice Dynamics* (Cambridge, Cambridge, 1993).

[89] V. Mazzacurati, G. Ruocco, and M. Sampoli, EPL (Europhysics Letters) **34**, 681 (1996), URL http://stacks.iop.org/0295-5075/34/i=9/a=681.

[90] J. Fabian, J. L. Feldman, C. S. Hellberg, and S. M. Nakhmanson, Phys. Rev. B **67**, 224302 (2003), URL http://link.aps.org/doi/10.1103/PhysRevB.67.224302.

[91] P. Sheng and M. Zhou, Science **253**, 539542 (1991), URL http://www.sciencemag.org/content/253/5019/539.abstract.

[92] J. T. Edwards and D. J. Thouless, Journal of Physics C: Solid State Physics **5**, 807 (1972), URL http://stacks.iop.org/0022-3719/5/i=8/a=007.

[93] W. Garber, F. M. Tangerman, P. B. Allen, and J. L. Feldman, Philosophical Magazine Letters **81**, 433439 (2001), URL http://www.tandfonline.com/doi/abs/10.1080/09500830110041666.

[94] N. Xu, V. Vitelli, M. Wyart, A. J. Liu, and S. R. Nagel, Phys. Rev. Lett. **102**, 038001 (2009), URL http://link.aps.org/doi/10.1103/PhysRevLett.102.038001.

[95] C. Kittel, Physical Review **75**, 974 (1949).

[96] G. A. Slack (Academic Press, 1979), vol. 34 of *Solid State Physics*, p. 1 71, URL http://www.sciencedirect.com/science/article/pii/S0081194708603598.

[97] Y. H. Lee, R. Biswas, C. M. Soukoulis, C. Z. Wang, C. T. Chan, and K. M. Ho, Phys. Rev. B **43**, 65736580 (1991), URL http://link.aps.org/doi/10.1103/PhysRevB.43.6573.

[98] M. S. Love and A. C. Anderson, Phys. Rev. B **42**, 18451847 (1990), URL http://link.aps.org/doi/10.1103/PhysRevB.42.1845.

[99] A. M. Bouchard, R. Biswas, W. A. Kamitakahara, G. S. Grest, and C. M. Soukoulis, Phys. Rev. B **38**, 1049910506 (1988), URL http://link.aps.org/doi/10.1103/PhysRevB.38.10499.

[100] P. G. Klemens, Proceedings of the Physical Society. Section A **68** (1955).

[101] J. L. Feldman, N. Bernstein, D. A. Papaconstantopoulos, and M. J. Mehl, Phys. Rev. B **70**, 165201 (2004), URL http://link.aps.org/doi/10.1103/PhysRevB.70.165201.

[102] M. E. Siemens, Q. Li, R. Yang, K. A. Nelson, E. H. Anderson, M. M. Murnane, and H. C. Kapteyn, Nature Materials **9**, 2630 (2010).